

## On the Mechanism of the Palladium(0)-Catalyzed Isomerization of Epoxides to Carbonyl Compounds

Sanjitha Kulasegaram and Robert J. Kulawiec\*,<sup>1</sup>

Department of Chemistry, Georgetown University

Washington, DC 20057-1227

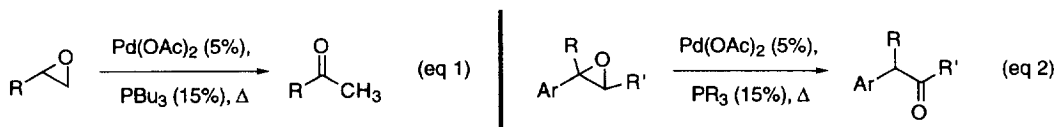
Received 8 August 1997; revised 4 November 1997; accepted 7 November 1997

**Abstract:** The isomerization of *trans*-3-methyl-2-(2-naphthyl)oxirane to 2-naphthylpropanone by Pd(OAc)<sub>2</sub>/PBu<sub>3</sub> in C<sub>6</sub>H<sub>6</sub> is first order in both epoxide and in palladium catalyst, with activation parameters of  $\Delta H^\ddagger = 12.5$  kcal/mol and  $\Delta S^\ddagger = -35.7$  e.u. A comparison of the isomerization rates of *trans*-3-methyl-2-(2-naphthyl)oxirane and *trans*-3-deuterio-3-methyl-2-(2-naphthyl)oxirane reveals a kinetic isotope effect ( $k_H/k_D$ ) of 1.01 ( $\pm 0.09$ ). The reaction rates in benzene and acetonitrile are very similar; however, changing from benzene to a hydrogen bond-donating solvent (*t*-BuOH) increases the reaction rate substantially. These observations are consistent with a mechanism involving: (1) turnover-limiting S<sub>N</sub>2 attack of Pd(0) at the benzylic position of the epoxide; (b) rapid  $\beta$ -hydride elimination to form a Pd(II) hydrido-enolate complex; and (c) fast reductive elimination to afford the ketone, with concomitant regeneration of the Pd(0) catalyst.

© 1998 Elsevier Science Ltd. All rights reserved.

### INTRODUCTION

The selective isomerization of one functional group into another by a transition metal catalyst is an atom-economical and synthetically useful process.<sup>2</sup> Prominent examples of isomerization via bond migration include the rearrangement of double bonds in unfunctionalized alkenes,<sup>3</sup> allylic amines<sup>4</sup> and allylic alcohols<sup>5</sup> to provide more highly-substituted alkenes, enamines and carbonyl compounds, respectively. Similarly, metal-catalyzed [3,3]-sigmatropic rearrangements are known.<sup>6</sup> Strained-ring compounds, encompassing both carbo- and heterocycles, also undergo metal-catalyzed isomerizations,<sup>7</sup> often resulting in major structural reorganizations. As part of our general research program aimed at developing synthetically useful transformations of small-ring heterocycles catalyzed by transition metal complexes, we have recently studied the isomerization of epoxides to carbonyl compounds<sup>8</sup> using a palladium(0) catalyst generated from Pd(OAc)<sub>2</sub> and tertiary phosphines. We have reported that palladium acetate/tributylphosphine catalytically isomerizes monoalkyl-substituted epoxides to methyl ketones (eq 1),<sup>9</sup> and that Pd(OAc)<sub>2</sub>/PR<sub>3</sub> (where R = Ph or *n*-Bu) rearranges aryl-substituted epoxides to benzylic aldehydes or ketones, depending on the substitution pattern (eq 2).<sup>10</sup> In both of these reactions, the

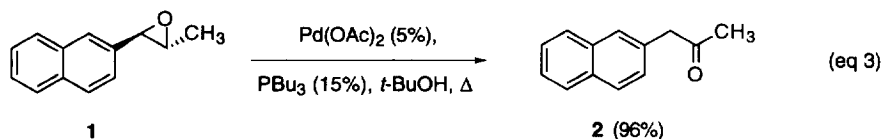


products are formed in high yield, under mild conditions, with complete chemoselectivity for the indicated functional group. In the reaction depicted in eq 2, epoxides with a variety of substitution patterns (R = R' = H; R = H, R' = CH<sub>3</sub>; R = CH<sub>3</sub>, R' = H; R = R' = CH<sub>3</sub> or (CH<sub>2</sub>)<sub>4</sub>) undergo isomerization rapidly, in nearly quantitative yields. Additionally, the catalyst tolerates a wide range of functional groups (such as olefin, nitrile,

enoate ester, alcohol and ketone) in the epoxide substrate. In order to understand more fully how the Pd(0) catalyst carries out such selective reactions, we have undertaken a mechanistic study of the isomerization of a prototypical aryl-substituted epoxide to a benzylic ketone, which we wish to describe in the present contribution. As discussed in detail below, our observations are consistent with a three-step mechanism involving turnover-limiting  $S_N2$  attack of Pd(0) at the benzylic position of the epoxide, rapid  $\beta$ -hydride elimination to form a Pd(II) hydrido-enolate complex, and rapid reductive elimination to form the ketone. Parts of this work have been communicated previously.<sup>11</sup>

## RESULTS

**Rate Law.** We chose the Pd(0)-catalyzed isomerization of *trans*-3-methyl-2-(2-naphthyl)oxirane (**1**) to 2-naphthylpropanone (**2**, eq 3) as our model reaction because it proceeds cleanly, rapidly and in high yield



(96%).<sup>10</sup> Although aryl-substituted epoxides isomerize efficiently in a variety of solvents, we chose benzene for our kinetics experiments. We commonly employ *t*-BuOH for synthetic reactions; however, benzene was judged to be preferable for kinetic studies because, as described below, the rate of the isomerization was inconveniently rapid in the protic solvent. As reported previously,<sup>9,10</sup> the isomerization reaction is carried out by generating the Pd(0) catalyst *in situ* from Pd(OAc)<sub>2</sub> and PBu<sub>3</sub> (3 equiv per Pd) in benzene, adding a solution of the catalyst to the epoxide, and heating until conversion to the carbonyl compound is complete. The reaction can be conveniently monitored using capillary GC, by removing aliquots periodically with a TLC pipette, filtering through silica gel, and integrating the area of the epoxide starting material (normalizing against internal hexadecane). Using an initial epoxide concentration of 0.026 M, a catalyst loading of 5 mol% Pd(0), and a constant temperature of 37 ( $\pm$  0.5) °C, a plot of  $\ln([1]_0/[1]_t)$  vs. time (Figure 1) gave a straight line ( $r^2 = 0.99$ )

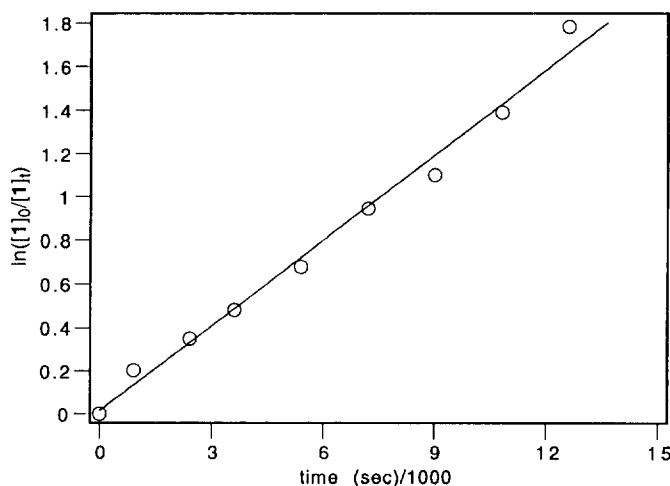


Figure 1: First-Order Plot for **1**  $\rightarrow$  **2**

for over two half-lives, indicating that, at least in the initial stages of the reaction, the isomerization rate is first-order in epoxide. From the slope of this line, a pseudo-first order rate constant of  $1.31 (\pm 0.05) \times 10^{-4} \text{ sec}^{-1}$  is obtained.

In order to determine the order of the reaction with respect to the palladium catalyst, a series of experiments was carried out in which the initial epoxide concentration ( $0.026 \text{ M}$ ) and temperature ( $37 \pm 0.5 \text{ }^\circ\text{C}$ ) were held constant, but the Pd(0) concentration was varied. Using catalyst concentrations ranging from  $6.6 \times 10^{-4} \text{ M}$  to  $3.1 \times 10^{-3} \text{ M}$  (2.5–12.5 mol%, relative to epoxide), values of the pseudo-first order rate constants were determined as described above, and are listed in Table 1. Again, in all cases, the first-order plots are linear over two to three half-lives. A plot of  $k_{\text{obs}}$  vs. catalyst concentration (Figure 2) is linear ( $r^2 = 0.97$ ), indicating that the isomerization reaction is also first order in [Pd(0)]. The slope of the line obtained in Figure 2 gives an absolute second-order rate constant of  $1.01 (\pm 0.10) \times 10^{-1} \text{ M}^{-1} \text{ sec}^{-1}$  at  $37 \text{ }^\circ\text{C}$ .

**Table 1. Dependence of Pseudo-First Order Rate Constant on Catalyst Concentration<sup>a</sup>**

[Pd(0)], M	$k_{\text{obs}}$ ( $\text{sec}^{-1}$ )/ $10^{-4}$	$r^2$
$6.6 \times 10^{-4}$	$0.99 \pm 0.05$	0.97
$1.3 \times 10^{-3}$	$1.31 \pm 0.05$	0.99
$1.9 \times 10^{-3}$	$1.87 \pm 0.05$	0.99
$2.5 \times 10^{-3}$	$2.77 \pm 0.12$	0.99
$3.1 \times 10^{-3}$	$3.33 \pm 0.16$	0.98

<sup>a</sup> T = 37°C; initial epoxide concentration = 0.026 M.

**Table 2. Dependence of Pseudo-First Order Rate Constant on Temperature<sup>a</sup>**

T ( $^\circ\text{C}$ )	$k_{\text{obs}}$ ( $\text{sec}^{-1}$ )/ $10^{-4}$	$r^2$
24	$0.68 \pm 0.03$	0.98
30	$0.96 \pm 0.05$	0.97
37	$1.31 \pm 0.05$	0.99
43	$2.09 \pm 0.22$	0.93
50	$4.40 \pm 0.35$	0.95

<sup>a</sup> initial epoxide concentration = 0.026 M; 5 mol% Pd(0).

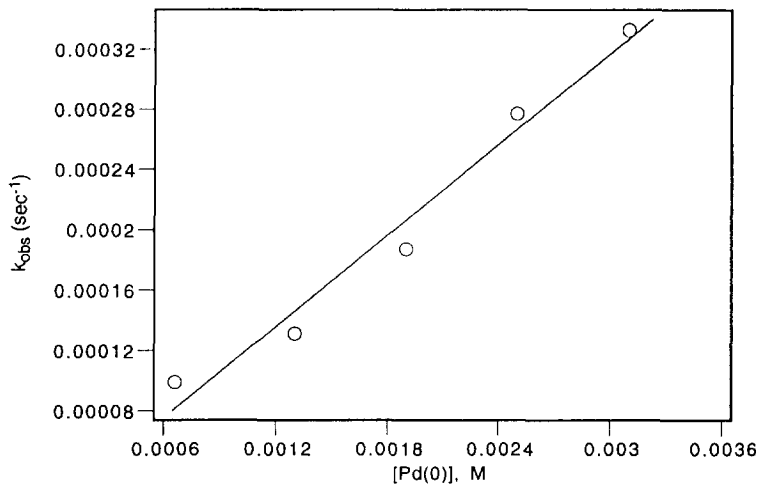


**Figure 2: Dependence of  $k_{\text{obs}}$  on [Pd(0)]**

**Activation Parameters.** Using a thermostatted bath, the pseudo-first order rate constants for the isomerization of **1** to **2** with 5 mol% Pd catalyst at five temperatures between  $24 \text{ }^\circ\text{C}$  and  $50 \text{ }^\circ\text{C}$  were measured using the method described above, and are listed in Table 2. A standard Eyring plot<sup>12</sup> of  $\ln(k/T)$  vs.  $1/T$  was

constructed (Figure 3); from the slope and intercept of this straight line ( $r^2 = 0.95$ ), activation parameters of  $\Delta H^\ddagger = 12.5 (\pm 1.6) \text{ kcal mol}^{-1}$  and  $\Delta S^\ddagger = -35.7 (\pm 5.3) \text{ cal mol}^{-1} \text{ K}^{-1}$  were calculated.

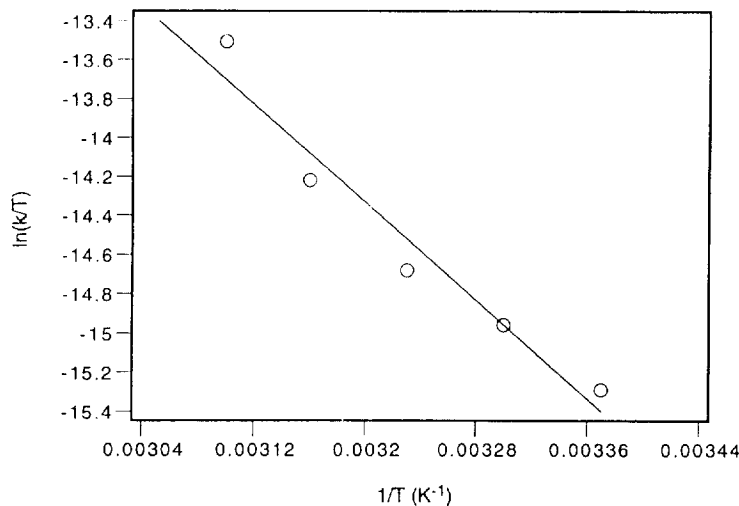


Figure 3: Eyring Plot for 1 → 2

**Solvent Effects.** In order to determine the influence of solvent properties on the rate of the isomerization reaction, we examined the rearrangement of epoxide **1** to ketone **2** as in eq 3 in three solvents of widely varying polarity: benzene, acetonitrile and *tert*-butyl alcohol. The pseudo-first order rate constants at 37 ( $\pm 0.5$ ) °C were determined as described above. The rate constants measured in benzene and acetonitrile are shown in Table 3. With *t*-BuOH, however, the reaction proceeded so rapidly at 37 °C that it was essentially complete within 10 minutes. Thus, assuming that the reaction in *t*-BuOH is also first-order in epoxide, and that the half-life is no greater than ten minutes, we can place a lower limit on the estimated pseudo-first order rate constant of  $1.2 \times 10^{-3} \text{ sec}^{-1}$ .

Table 3. Dependence of Pseudo-First Order Rate Constant on Solvent<sup>a</sup>

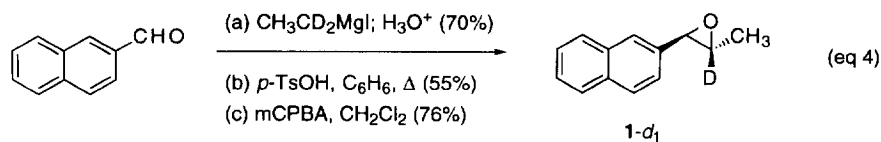
solvent	$\epsilon^b$	$k_{\text{obs}} (\text{sec}^{-1})/10^{-4}$	$r^2$
benzene	2.27	$1.31 \pm 0.05$	0.97
acetonitrile	35.94	$1.42 \pm 0.07$	0.98
<i>tert</i> -butyl alcohol	12.47	$\geq 12$	—

<sup>a</sup> T = 37 °C; initial epoxide concentration = 0.026 M; 5 mol% Pd(0).

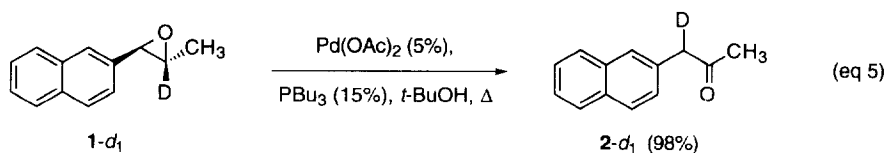
<sup>b</sup> Dielectric constant, measured at 25°C (from ref. 24).

**Kinetic Isotope Effect.** The isomerization reaction of **1** to **2** appears to involve the net migration of a hydrogen from C3 of the epoxide substrate to C1 of the product ketone (eq 3). In order to determine whether such apparent hydrogen transfer occurs cleanly, and to investigate whether cleavage of this C—H bond occurs in the turnover-limiting step of the isomerization reaction, we synthesized *trans*-3-deuterio-3-methyl-2-(2-naphthyl)oxirane (**1-d<sub>1</sub>**), as depicted in eq 4, and investigated its reactivity. The labeled compound was

prepared by the same series of reactions used to synthesize the unlabeled analog;<sup>10</sup> deuterium was introduced simply by employing 1,1-dideuterioethyl iodide in the first step of the sequence, rather than ethyl bromide.



Reaction of labeled epoxide **1-*d*<sub>1</sub>** under standard conditions (5 mol%  $\text{Pd}(\text{OAc})_2$ , 15 mol%  $\text{PBu}_3$ , *t*-BuOH, reflux, 10 min) led to the clean and near-quantitative formation of labeled ketone **2-*d*<sub>1</sub>** (98%, eq 5), in



which the deuterium is present only at C1. Under prolonged reaction times, partial loss of deuterium occurred to afford mixtures of **2-*d*<sub>1</sub>** and unlabeled **2**, as determined by <sup>13</sup>C NMR; however, a simple NMR tube experiment demonstrated that addition of  $\text{D}_2\text{O}$  (1 equiv per epoxide, in  $\text{C}_6\text{D}_6$ ) completely inhibits deuterium loss.

The relative isomerization rates of the labeled and unlabeled epoxides were determined by measuring rate constants, as described above, in parallel kinetic runs, using the same catalyst stock solution and temperature control bath ( $37 \pm 0.5^\circ\text{C}$ ), but in separate reaction flasks. The linear plots obtained from standard first-order treatment of the kinetic data are depicted in Figure 4. From the slopes of these lines, pseudo-first order rate constants of  $1.34 (\pm 0.05) \times 10^{-4} \text{ sec}^{-1}$  ( $r^2 = 0.99$ ) and  $1.33 (\pm 0.07) \times 10^{-4} \text{ sec}^{-1}$  ( $r^2 = 0.98$ ) were calculated for the unlabeled (**1**) and labeled (**1-*d*<sub>1</sub>**) epoxides, respectively. From these values, a kinetic isotope effect of  $k_{\text{H}}/k_{\text{D}} = 1.01 (\pm 0.09)$  was calculated.

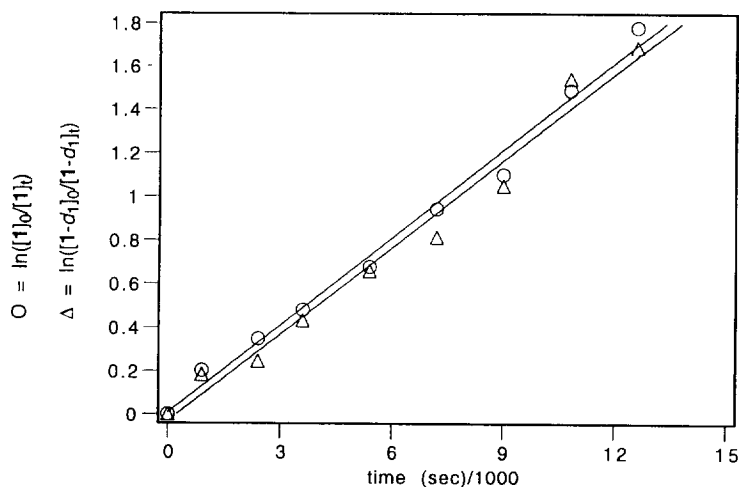


**Figure 4: First-Order Plots for **1** (O) and **1-*d*<sub>1</sub>** ( $\Delta$ )**

## DISCUSSION

**Proposed Mechanism.** Taking into consideration the results of the mechanistic experiments described above, as well as the mechanisms previously determined for related epoxide isomerization reactions<sup>8b</sup> and our knowledge of the fundamental chemistry of palladium,<sup>13</sup> we propose the mechanistic scenario depicted in Figure 5 below, which is consistent with our experimental data. The catalytic cycle comprises three fundamental steps. The first (and turnover-limiting) step is the nucleophilic attack of an electron-rich palladium(0) complex at the benzylic position of the epoxide, in an S<sub>N</sub>2-like process. This reaction results in the formation of a ring-opened, zwitterionic, β-alkoxyalkylpalladium(II) intermediate. The second step involves rapid β-hydride elimination in the ring-opened intermediate, yielding a hydridopalladium(II) enolate complex. Finally, rapid C-H reductive elimination affords the observed ketone product, and regenerates the Pd(0)-tributylphosphine complex as the active catalyst. In the following discussion, we will consider how each of our experimental findings supports this scenario.

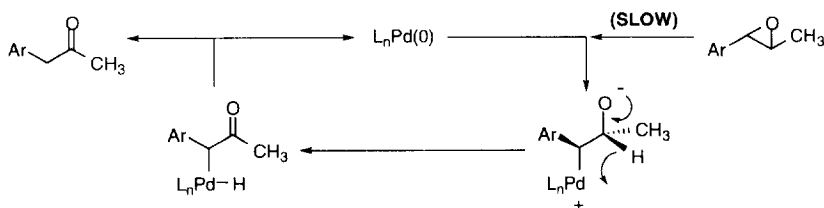


Figure 5: Proposed Isomerization Mechanism

**Rate Law.** The data depicted in Figure 1 demonstrate that the isomerization reaction is first-order in epoxide concentration over two to three half-lives of the reaction. Varying the amount of catalyst shows that the observed pseudo-first order rate constants, measured over an approximately five-fold variation in catalyst concentration, are linearly dependent on the concentration of Pd(0) (as depicted in Figure 2), indicating that the reaction is also first-order in palladium. The y-intercept of the  $k_{\text{obs}}$  vs. [Pd(0)] graph is zero, within experimental error ( $k_{\text{obs}}$  at [Pd(0)] = 0 is  $1.47 (\pm 2.01) \times 10^{-5} \text{ sec}^{-1}$ ), indicating that there are no competing non-catalyzed isomerization pathways. This point has also previously been demonstrated by a control experiment:<sup>10</sup> refluxing a solution of **1** in *t*-BuOH for 72 h gave no observable isomerization; unreacted **1** was recovered in 96% yield. Since the graph in Figure 2 corresponds to the equation  $k_{\text{obs}} = k_2[\text{Pd}(0)]$ , the slope is equal to the actual second-order rate constant:  $k_2 = 1.01 (\pm 0.10) \times 10^{-1} \text{ M}^{-1} \text{ sec}^{-1}$  at 37 °C.

The overall rate law deduced from the kinetics experiments described in Table 1, i.e.,  $-\text{d}[\mathbf{1}]/\text{dt} = k_2[\mathbf{1}][\text{Pd}(0)]$ , demonstrates that the turnover-limiting step is bimolecular,<sup>14a</sup> involving both the epoxide and a palladium complex.<sup>15</sup> Since the formation of a ketone in the isomerization reaction obviously requires cleavage of the benzylic C—O bond, it is reasonable to postulate an oxidative addition reaction<sup>16</sup> between the Pd(0) catalyst and the epoxide, forming a Pd(II) intermediate, as the first step. Such oxidative addition processes normally show bimolecular kinetics, as we see in the present case. Furthermore, the activation parameters, in particular the large negative entropy of activation ( $\Delta S^\ddagger = -35.7 \text{ cal/mol K}$ ), are fully consistent with an associative process in the turnover-limiting step. For example, the enthalpies of activation for the bimolecular oxidative addition of iodomethane to  $\text{IrCl}(\text{CO})(\text{PPh}_3)_2$ ,<sup>17</sup>  $\text{Cp}(\text{CO})\text{Co}(\text{PPh}_3)$ ,<sup>18</sup>  $\text{Cp}(\text{CO})\text{Rh}(\text{PPh}_3)$ <sup>18</sup> and  $\text{PtPh}_2(\text{bipy})$ <sup>19</sup> all fall between -31 and -51 cal/mol K. Likewise, values measured for the addition of H<sub>2</sub>,<sup>17</sup> O<sub>2</sub><sup>17</sup> and benzyl bromide<sup>20</sup> to  $\text{IrCl}(\text{CO})(\text{PPh}_3)_2$  range from -21 to -39 cal/mol K. Clearly, large and negative values of  $\Delta S^\ddagger$  are indicative of a bimolecular, associative reaction.

**Mechanism of Oxidative Addition.** The values of the activation parameters obtained above clearly indicate an associative process in the turnover-limiting step; however, they do not allow one to distinguish between an  $S_N2$  oxidative addition mechanism and a three-center mechanism (Figure 6).<sup>16,21</sup> We favor the

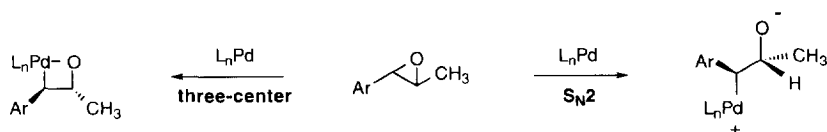
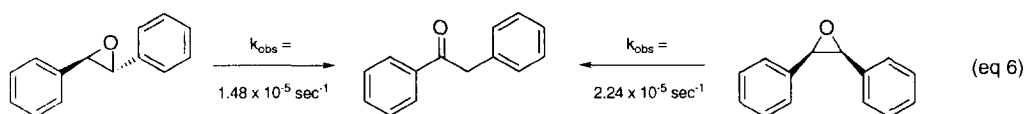
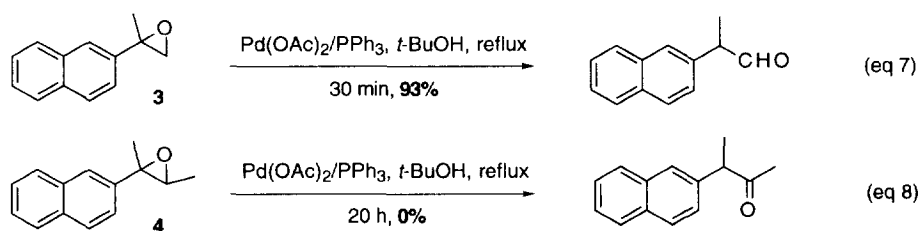


Figure 6: Possible Oxidative Addition Pathways

former pathway (which has previously been identified in oxidative addition reactions of Pd(0)<sup>16,22</sup>) for three major reasons. First, the rate of the reaction is sensitive to steric factors, consistent with an  $S_N2$  process. We previously reported that the rate of isomerization of *cis*-stilbene oxide to deoxybenzoin is approximately 50% greater than that of *trans*-stilbene oxide (eq 6),<sup>10</sup> and attributed this difference to the greater degree of steric



hindrance encountered in a backside-approach trajectory in the *trans* isomer. If a hypothetical three-center mechanism (i.e., concerted front-side insertion of Pd(0) into the C—O bond) were operative, there would seem to be much less difference in steric hindrance between the *cis*- and *trans*-isomers, as the phenyl rings would be located on the opposite face of the substrate relative to the direction of attack. Although the relief of ring strain would also be greater in the *cis* isomer, it is clear that such relief would be more pronounced in an  $S_N2$  mechanism, which results in an acyclic intermediate, than in a three-center mechanism, which forms a cyclic (and more conformationally restricted) intermediate. Other, more qualitative, examples demonstrating the dependence of isomerization rate on steric factors include our prior observation that both *cis*- and *trans*-stilbene oxide isomerize much more rapidly than 1,1-diphenyloxirane. Thus, reaction of *cis*-stilbene oxide with 5% Pd(OAc)<sub>2</sub>/PBu<sub>3</sub> in refluxing *t*-BuOH afforded a 97% yield of deoxybenzoin in 10 minutes; however, exposure of 1,1-diphenyloxirane to identical reaction conditions for 24 hours gave diphenylacetaldehyde in a mere 3% yield.<sup>10</sup> Similarly, one can compare the isomerization rates of 2-methyl-2-(2-naphthyl)oxirane (**3**) and *trans*-2,3-dimethyl-2-(2-naphthyl)oxirane (**4**) under identical conditions (5% Pd(OAc)<sub>2</sub>/PPh<sub>3</sub>, refluxing *t*-BuOH; eqs 7 and 8). The former substrate rearranged to give 2-(2-naphthyl)propanal in 93% yield after 30 minutes, while



the latter, after 20 h reflux using the same catalyst, gave *none of the expected isomerization product whatsoever*.<sup>10, 23</sup> Clearly, the steric influence of the additional alkyl substituent will be felt most strongly when

the Pd(0) catalyst approaches *syn* to the methyl group (i.e., via backside approach in an S<sub>N</sub>2 pathway) rather than *anti* to it (i.e., via frontside approach in a three-center mechanism).

A second argument in favor of an S<sub>N</sub>2 oxidative addition mechanism arises from the observed dependence of the isomerization rate on the nature of the solvent employed, as summarized in Table 3. It is well known that reactions involving charge separation in the transition state are accelerated in polar solvents.<sup>14b,24</sup> Although we observe a marked rate variation in different solvents, the rates do not correlate directly with solvent polarity, as expressed in the dielectric constants shown in Table 3. The isomerization rates in acetonitrile and benzene are equal, within experimental error; however, the rate of reaction is much greater in *tert*-butyl alcohol, a solvent with a dielectric constant that is actually less than that of acetonitrile. We explain this seemingly anomalous finding by noting that *t*-BuOH differs from the other two solvents tested in that it is capable of donating a hydrogen bond (i.e., X<sup>-</sup>⋯H—O—*t*-Bu).<sup>25</sup> Thus, we rationalize the greater reaction rate in this solvent by proposing that the charge separation which develops as the C—O bond of the epoxide lengthens in the transition state of the turnover-limiting S<sub>N</sub>2 attack is *stabilized by hydrogen-bonding with the protic solvent*, as illustrated in Figure 7. Such stabilization lowers the energy of the transition state, thereby

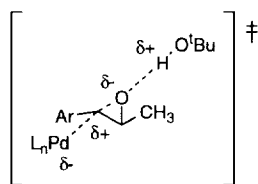


**Figure 7: Proposed Transition State for Turnover-Limiting Step**

increasing the reaction rate in *t*-BuOH relative to the non-hydroxylic solvents C<sub>6</sub>H<sub>6</sub> and MeCN. It is important to note that the alternative oxidative addition mechanism (i.e., three-center, front-side insertion into the C—O bond) is not expected to involve nearly as much developing charge separation in the transition state as in an S<sub>N</sub>2 process, and thus would not be expected to undergo significant stabilization by hydrogen-bonding. The rates of oxidative addition of iodomethane to PtPh<sub>2</sub>(bipy) and IrCl(CO)(PPh<sub>3</sub>)<sub>2</sub>, both of which are known to react via the S<sub>N</sub>2 mechanism, show a strong dependence on solvent polarity.<sup>26</sup> For both complexes, the second order rate constants measured in acetone are approximately six times greater than those determined in benzene. Unfortunately, these studies did not include any protic solvents, so a direct comparison with our results is not possible.

Finally, one should also consider the stereoelectronic requirements of the subsequent β-hydride elimination step. If the oxidative addition reaction were to occur via a three-center insertion mechanism, the resulting product would be a metallaoxetane. It is firmly established that β-H elimination occurs preferentially from a *syn*-coplanar conformation of the M—C—C—H moiety.<sup>27</sup> However, the structure of a metallaoxetane places β-substituents quite far from the metal center. For example, in the X-ray crystal structure of the rhodaoxetane *mer*-(PMe<sub>3</sub>)<sub>3</sub>BrRh(η<sup>2</sup>-{*C,O*}-OCH<sub>2</sub>C(CH<sub>3</sub>)<sub>2</sub>) reported by Milstein and colleagues,<sup>28</sup> the torsional angles between the Rh—C bond and the two C—CH<sub>3</sub> bonds are -118.0° and 121.2°. Thus, it is difficult to see how β-H elimination might occur directly from such a conformationally restricted metallacycle. Of course, elimination could take place *after* an initially-formed metallaoxetane undergoes ring-opening to form the β-alkoxyalkylpalladium intermediate proposed above. However, it would then be difficult to reconcile the simultaneous observations of bimolecularity (from the rate law and activation parameters) *and* development of charge separation (from the solvent dependence studies) in the transition state of the turnover-limiting step.

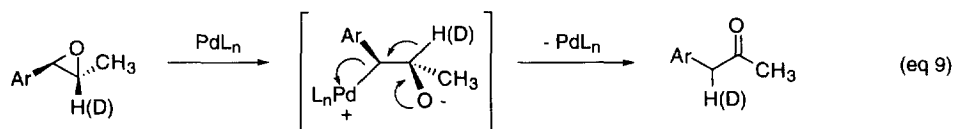


As a final note on the subject, we recognize that it is quite tempting to propose a simple stereochemical experiment<sup>16,22</sup> to distinguish between the two oxidative addition mechanisms suggested in Figure 6, i.e., investigation of the stereochemistry of ring-opening using an enantiomerically enriched version of a chiral, 2,2-disubstituted epoxide such as **3** or **4**. We did not attempt such an experiment because our previous work clearly demonstrated that the benzylic aldehydes and ketones formed in the isomerization of aryl-substituted epoxides readily enolize under the reaction conditions. For example, we have reported that treatment of styrene oxide with Pd(OAc)<sub>2</sub>/PBU<sub>3</sub> for extended periods results in a tandem epoxide isomerization/aldol condensation reaction to form 2,4-diphenyl-2-butenal in good yield.<sup>29</sup> Thus, any stereochemical information regarding retention or inversion of configuration at the benzylic position during the isomerization reaction would in all likelihood be lost due to rapid enolization.

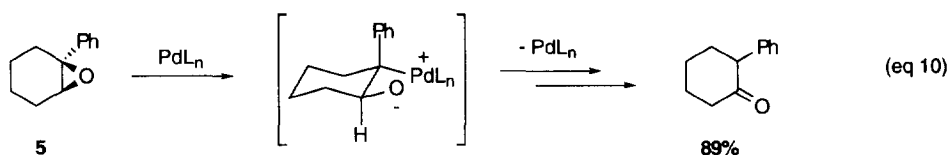
**Deuterium Labeling Studies.** The preparative-scale isomerization of the labeled epoxide **1-d<sub>1</sub>** (eq 5) demonstrates that the deuterium atom on C3 of the epoxide substrate migrates cleanly to the C1 position of the ketone product, **2-d<sub>1</sub>**. Evidence for the location of the deuterium atoms in **1-d<sub>1</sub>** and **2-d<sub>1</sub>** arises from the <sup>13</sup>C{<sup>1</sup>H} NMR spectra: in both cases, the deuterated carbon appears as a 1:1:1 triplet, with coupling constants (<sup>1</sup>J<sub>CD</sub>) of 27 Hz and 32 Hz, respectively. This migration is consistent with our proposed mechanism, in which the hydrogen atom in the β-position of the β-alkoxyalkylpalladium(II) intermediate is transferred to the benzylic position of the product ketone. The slight loss of deuterium noted under prolonged reaction conditions in either *t*-BuOH or benzene is attributed to enolization of the benzylic ketone under the reaction conditions,<sup>29</sup> and subsequent proton exchange with the protic solvent (or with traces of H<sub>2</sub>O present when non-hydroxylic solvents are employed). This hypothesis is substantiated by two observations. First, the extent of deuterium loss is time-dependent: qualitatively, longer reaction times result in greater loss of deuterium. Second, the presence of D<sub>2</sub>O (1 equiv per epoxide) inhibits deuterium loss completely, as determined by an experiment in which the isomerization of **1-d<sub>1</sub>** was monitored by NMR (C<sub>6</sub>D<sub>6</sub>, room temperature).

The kinetic isotope effect of 1.01 (± 0.09), calculated from a direct comparison of the isomerization rates of **1** and **1-d<sub>1</sub>**, demonstrates unambiguously that cleavage of the C3—H(D) bond does not occur in or prior to the turnover-limiting step of the reaction.<sup>14c</sup> Within the context of our mechanistic rationale (Figure 5), this observation is consistent with the proposal that the oxidative addition (step 1) is turnover-limiting, not the β-hydride elimination (step 2). For comparison, the kinetic isotope effect for rate-determining β-hydride elimination in the octyliridium(I) complex (CO)(PPh<sub>3</sub>)<sub>2</sub>IrCH<sub>2</sub>CHDR (R = *n*-C<sub>6</sub>H<sub>13</sub>) is 2.28 (± 0.20), as reported by Schwartz.<sup>30</sup> Similar values have been observed in β-hydride eliminations of organoaluminum(III) compounds.<sup>31</sup>

An alternative mechanistic possibility for the C—H bond cleavage step is a concerted 1,2-hydride migration with concomitant expulsion of Pd(0) (eq 9). We cannot firmly rule out this possibility, but we favor



the pathway indicated in Figure 5 for two reasons. First, the facile isomerization of bicyclic epoxide **5** to 2-phenylcyclohexanone under our standard reaction conditions (eq 10)<sup>10</sup> is more consistent with a β-elimination pathway than a 1,2-hydride migration. In the postulated ring-opened intermediate, the formation of which is strongly supported by our solvent studies (*vide supra*), the palladium and the β-hydrogen are not in the anti-periplanar conformation required for a concerted hydride migration, as in eq 9. In fact, they are much closer to (although not perfectly aligned in) the syn-coplanar conformation preferred for β-hydride elimination.<sup>27</sup>



Second, and perhaps more convincingly,  $\beta$ -hydride elimination in coordinatively unsaturated alkylpalladium(II) complexes is ubiquitous in the organometallic chemistry of palladium.<sup>13,27</sup> It is difficult to understand why an alkylpalladium intermediate bearing a  $\beta$ -hydrogen would *not* undergo such elimination. In any event, even if the C—H cleavage occurs by the hydride migration pathway of eq 9, the kinetic isotope effect discussed above firmly rules out the possibility that this step is turnover-limiting.

**The Final Step.** The intermediate formed after the  $\beta$ -hydride elimination step is a Pd(II) hydrido-enolate complex.<sup>32</sup> We depict this enolate intermediate as carbon-bound, for convenience; however, we have no direct information concerning its structure, and it might alternatively exist in an oxygen-bound form. Relatively few palladium(II) complexes bearing unstabilized enolate ligands have been characterized. In 1990, Bergman and Heathcock reported the preparation of cyclopentadienylpalladium(II) enolate complexes  $\text{Cp}(\text{PPh}_3)\text{Pd}(\text{CHRC}(=\text{O})\text{R}')$  ( $\text{R} = \text{H}, \text{CH}_3$ ;  $\text{R}' = t\text{-Bu}, \text{Ph}, \text{OMe}$ ), which were assigned carbon-bound structures, based on comparison of their spectroscopic properties to those of structurally characterized nickel(II) analogs.<sup>33</sup> Similarly, Floriani described the oxidative addition of  $\alpha$ -chloroacetophenone to  $\text{Pd}(\text{PPh}_3)_4$  to form the structurally characterized *trans*- $(\text{PPh}_3)_2\text{PdCl}(\text{CH}_2\text{C}(=\text{O})\text{Ph})$ , in which the enolate ligand also coordinates via carbon.<sup>34</sup> In contrast, enolate complex intermediates formed *in situ* by reaction of palladium(II) complexes and silyl enol ethers have been assigned O-bound structures, based primarily on spectroscopic evidence.<sup>35</sup> In any event, it is likely that reductive elimination in our reaction occurs from a carbon-bound enolate intermediate, considering the principle of least motion.

Our kinetic and isotope labeling studies are consistent with a rapid product-forming reductive elimination step. In 1982, Milstein reported the catalytic isomerization of propylene oxide to acetone, and styrene oxide to acetophenone, by  $\text{RhCl}(\text{PMe}_3)_3$ .<sup>36</sup> A mechanistic study of this reaction demonstrated a pathway strikingly similar to that proposed in Figure 5. In contrast to our results, however, Milstein found that phosphine dissociation prior to reductive elimination was the turnover-limiting step. This conclusion was based on the observations that (a) the hydridorhodium enolate complexes formed after step 2, *mer,cis*- $(\text{PMe}_3)_3\text{RhH}(\text{CH}_2\text{C}(=\text{O})\text{R})\text{Cl}$ , were isolable; and (b) reductive elimination of  $\text{RC}(=\text{O})\text{CH}_3$  from the hydrido-enolate complexes was retarded by addition of excess  $\text{PMe}_3$ , and showed a positive entropy of activation. The difference in rates of reductive elimination in the two catalytic cycles probably arises from the greater kinetic lability of Pd(II) ( $d^8$ ) compared to Rh(III) ( $d^6$ ).

## CONCLUSIONS

In summary, we have shown that the isomerization of an aryl-substituted epoxide (1) to the benzylic ketone (2) with a Pd(0) catalyst is first order in both substrate and catalyst, and shows a large negative entropy of activation, consistent with a bimolecular oxidative addition reaction as the turnover-limiting step. In addition, the observed kinetic isotope effect of unity precludes the subsequent C—H cleavage step (most likely a traditional  $\beta$ -hydride elimination) from being turnover-limiting. An increased reaction rate in *t*-BuOH, a hydrogen bond-donating solvent, argues for an  $\text{S}_{\text{N}}2$ -type oxidative addition mechanism. Although our studies

were limited to a single epoxide, we suggest that the similarity between the reaction profiles of **1** and those of other epoxides<sup>9,10</sup> implies that a similar mechanism operates. We are continuing to explore the diverse reaction pathways available to epoxides in the presence of low-valent metal complexes, and to exploit them to synthetic advantage.

## EXPERIMENTAL SECTION

**General Considerations:** The general experimental and spectroscopic techniques employed in this study have been described in detail previously.<sup>10</sup> NMR spectra were measured at 270 MHz (<sup>1</sup>H) and 67.9 MHz (<sup>13</sup>C) in CDCl<sub>3</sub>, unless otherwise indicated. Reaction temperatures were controlled to  $\pm 0.5$  °C using a VWR Model 1130 temperature control bath. Solvents and reagents were purchased from commercial suppliers, and used as received.

**Kinetic Experiments:** A representative kinetic experiment is as follows. Palladium(II) acetate (0.56 mg, 2.5  $\mu$ mol; from Strem Chemicals, recrystallized from benzene prior to use) was added to an oven-dried 5 mL vial, which was capped with a septum and purged with N<sub>2</sub>. To this was added deoxygenated benzene (0.5 mL) and PBu<sub>3</sub> (1.9  $\mu$ L, 7.5  $\mu$ mol), to generate a bright yellow solution of the Pd(0) catalyst. In a separate Schlenk flask, *trans*-3-methyl-2-(2-naphthyl)oxirane<sup>9</sup> (**1**, 9.2 mg, 0.050 mmol) and hexadecane (2.0  $\mu$ L) were dissolved in deoxygenated benzene (1.5 mL), and the flask was placed in the temperature control bath (previously equilibrated at 30 °C). After 30 minutes, a 0.46 mL aliquot of the catalyst solution was withdrawn from the catalyst vial and added to the Schlenk flask ( $t = 0$ ), resulting in a final epoxide concentration of 0.026 M, and a final catalyst concentration of  $1.3 \times 10^{-3}$  M (5 mol% relative to **1**). Aliquots were withdrawn periodically through the septum using a TLC pipet and a 16-gauge needle, and were filtered through a plug of silica gel and analyzed by GC. The integrated area of the epoxide was normalized by dividing it by the integrated area of the hexadecane internal standard. The data were subjected to a standard first-order kinetic treatment by plotting  $\ln([1]_0/[1]_t)$  vs. time, as depicted in Figure 1; using the plotting program MacCurveFit (version 1.1), a slope was calculated, from which the pseudo-first order rate constant was determined. The uncertainty on the rate constant was estimated by least-squares curve fitting available on the same program. For the catalyst concentration dependence experiments summarized in Table 1, the concentration of Pd(0) was varied simply by changing the amounts of Pd(OAc)<sub>2</sub> and PBu<sub>3</sub> used in preparing the catalyst solution. For the temperature dependence experiments summarized in Table 2, the thermostatted bath was pre-equilibrated at the indicated temperature. For the solvent dependence experiments summarized in Table 3, the indicated solvent was substituted in place of benzene.

**Synthesis of *trans*-3-deuterio-3-methyl-2-(2-naphthyl)oxirane (**1-d<sub>1</sub>**):** A solution of CH<sub>3</sub>CD<sub>2</sub>MgI was prepared from 1,1-dideuterioethyl iodide (1.5 g, 9.5 mmol; Cambridge Isotopes) and Mg (0.277 g, 11.0 mmol) in ether (10 mL). After completion of reaction, the solution was cooled to 0 °C and treated dropwise with a solution of 2-naphthaldehyde (0.74 g, 4.8 mmol) in ether (10 mL). The mixture was warmed to room temperature over one hour (at which point TLC showed no aldehyde) and poured onto ice. The phases were separated, and the organic layer was washed with satd. NaHSO<sub>4</sub> (20 mL), satd. NaHCO<sub>3</sub> (3 x 20 mL) and brine (20 mL). After drying (MgSO<sub>4</sub>) and evaporation, the crude product was purified by flash chromatography (6:1 hexane-ethyl acetate, R<sub>f</sub> = 0.26) to afford 623 mg (70%) of 2,2-dideuterio-1-(2-naphthyl)-1-propanol, m.p. = 32–34 °C. IR (film): 3357, 3055, 2962, 2874, 2217, 2187, 2118, 1919, 1648, 1617, 1509, 1454, 1378, 1310, 1270, 1169, 1124, 1053, 1018, 997, 894, 857, 819, 748. <sup>1</sup>H NMR:  $\delta$  7.85–7.45 (m, 7H), 4.76 (s, 1H), 1.95 (d, J = 3.4 Hz, 1H), 0.93 (s, 3H). <sup>13</sup>C NMR:  $\delta$  141.8, 133.2, 132.9, 128.0, 127.8, 127.5, 125.9, 125.6, 124.6, 124.0, 75.8, 30.9 (quint, <sup>1</sup>J<sub>CD</sub> = 19 Hz), 9.9. MS: 188 (M<sup>+</sup>, 76.6), 169 (26.0), 157 (100.0), 129

(98.5), 115 (6.5), 102 (9.7), 77 (16.5), 63 (5.7), 51 (5.4). HRMS: calcd. for  $C_{13}H_{12}D_2O$  ( $M^+$ )  $m/z$  188.1171, found 188.1161. A solution of this alcohol (620 mg, 3.3 mmol) and *p*-toluenesulfonic acid hydrate (63 mg, 0.33 mmol) in benzene (10 mL) was refluxed for 30 minutes. After cooling, the mixture was washed with satd.  $NaHCO_3$  (10 mL) and brine (10 mL), dried ( $MgSO_4$ ), and evaporated. The crude product was chromatographed (hexane,  $R_f = 0.56$ ) to give 309 mg (55%) of (*E*)-2-deuterio-1-(2-naphthyl)-1-propene, m.p. = 42–44 °C. IR (film): 3058, 2951, 2858, 2238, 1939, 1915, 1627, 1598, 1509, 1460, 1378, 1270, 1178, 1150, 1125, 1017, 948, 908, 851, 815, 748, 697.  $^1H$  NMR:  $\delta$  7.85–7.45 (m, 7H), 6.55 (s, 1H), 1.98 (s, 3H).  $^{13}C$  NMR:  $\delta$  135.4, 133.7, 132.6, 131.1, 131.0, 127.8 (t,  $^1J_{CD} = 15$  Hz), 126.0, 125.3, 125.1, 125.0, 123.6, 123.5, 18.5. MS: 170 ( $M^+$ , 51.9), 153 (86.5), 141 (33.6), 128 (21.8), 115 (37.9), 102 (6.6), 84 (63.8), 63 (13.4), 51 (5.4). HRMS: calcd. for  $C_{13}H_{11}D$  ( $M^+$ )  $m/z$  169.1002, found 169.1005. A solution of this alkene (300 mg, 1.7 mmol) in  $CH_2Cl_2$  (10 mL) was cooled to 0 °C, treated with mCPBA (496 mg, 73.4% pure, 2.11 mmol) and allowed to warm to room temperature over 2 hours. The mixture was then diluted with ether (10 mL), washed with satd.  $Na_2S_2O_3$  (3 x 10 mL), satd.  $NaHCO_3$  (3 x 10 mL), 5% NaOH (3 x 10 mL) and brine (10 mL), dried ( $MgSO_4$ ), and evaporated. Flash chromatography (6:1 hexane-ethyl acetate,  $R_f = 0.61$ ) gave 250 mg (76%) of *trans*-3-deuterio-3-methyl-2-(2-naphthyl)oxirane, m.p. = 55–57 °C. IR (film): 3049, 2929, 2854, 2224, 1958, 1928, 1599, 1511, 1460, 1410, 1377, 1345, 1282, 1123, 1075, 951, 908, 813, 741.  $^1H$  NMR:  $\delta$  7.81–7.28 (m, 7H), 3.72 (s, 1H), 1.48 (s, 3H).  $^{13}C$  NMR:  $\delta$  135.2, 133.2, 133.1, 128.1, 127.7, 126.1, 125.9, 124.9, 124.8, 122.9, 59.7, 58.5 (t,  $^1J_{CD} = 27$  Hz), 17.7. MS: 186 ( $M^+$ , 37.7), 170 (46.4), 155 (88.6), 142 (96.8), 127 (43.6), 116 (60.9), 101 (6.7), 89 (17.1), 77 (14.7), 63 (19.7), 51 (8.2), 43 (30.9). HRMS: calcd. for  $C_{13}H_{11}DO$  ( $M^+$ )  $m/z$  185.0951, found 185.0949.

**Synthesis of 1-deuterio-1-(2-naphthyl)propanone (2-*d*<sub>1</sub>):** To a solution of  $Pd(OAc)_2$  (3.0 mg, 13.5  $\mu$ mol) in 0.5 mL deoxygenated *t*-BuOH in a Schlenk flask under  $N_2$  was added  $PBu_3$  (10.1  $\mu$ L, 40.5  $\mu$ mol) via microliter syringe. After formation of the bright yellow color indicative of Pd(0) (ca. 2 minutes), *trans*-3-deuterio-3-methyl-2-(2-naphthyl)oxirane (50 mg, 0.269 mmol) was added. The homogeneous solution was refluxed under  $N_2$  for 10 minutes, at which point TLC and GC indicated complete consumption of starting material. The reaction mixture was chromatographed directly (silica gel, 6:1 hexane-ethyl acetate,  $R_f = 0.38$ ) to give 49.0 mg (98%) of 1-deuterio-1-(2-naphthyl)propanone. IR (film): 3059, 2978, 2935, 2866, 2109, 2067, 1948, 1713, 1629, 1598, 1508, 1468, 1420, 1354, 1274, 1219, 1177, 1118, 1020, 958, 900, 860, 817, 748.  $^1H$  NMR:  $\delta$  7.81–7.28 (m, 7H), 3.81 (s, 1H), 2.16 (s, 3H).  $^{13}C$  NMR:  $\delta$  206.4, 133.4, 132.3, 131.6, 128.3, 127.9, 127.6, 127.5, 127.3, 126.1, 125.7, 50.8 (t,  $^1J_{CD} = 32$  Hz), 29.3. MS: 186 ( $M^+$ , 57.7), 169 (2.9), 153 (7.2), 142 (100), 116 (80.4), 102 (5.7), 89 (26.7), 75 (14.6), 63 (32.9), 51 (12.9). HRMS: calcd. for  $C_{13}H_{11}DO$  ( $M^+$ )  $m/z$  185.0951, found 185.0945.

## ACKNOWLEDGMENTS

The authors thank Georgetown University for financial support of this research, and Profs. Robert E. Bachman and Colby A. Foss, Jr., for helpful discussions. The authors also thank Dr. Lewis Pannell of the National Institutes of Health for measuring the high-resolution mass spectra.

## REFERENCES AND NOTES

1. Author to whom correspondence should be addressed. e-mail: kulawiec@guvax.georgetown.edu. fax: (202) 687-6209.

2. Davies, S. G. *Organotransition Metal Chemistry: Applications to Organic Synthesis*; Pergamon: Oxford, 1982; Chapter 7.
3. Parshall, G. W.; Ittel, S. D. *Homogeneous Catalysis*, 2nd ed.; Wiley and Sons: New York, 1992; Chapter 2.
4. For a recent example, see: Tani, K.; Yamagata, T.; Akutagawa, S.; Kumobayashi, H.; Taketomi, T.; Takaya, H.; Miyashita, A.; Noyori, R.; Otsuka, S. *J. Am. Chem. Soc.* **1984**, *106*, 5208-5217.
5. For recent examples, see: (a) McGrath, D. V.; Grubbs, R. H. *Organometallics* **1994**, *13*, 224-235. (b) Trost, B. M.; Kulawiec, R. J. *J. Am. Chem. Soc.* **1993**, *115*, 2027-2036. (c) Bergens, S. H.; Bosnich, B. *J. Am. Chem. Soc.* **1991**, *113*, 958-967.
6. Overman, L. E. *Angew. Chem., Int. Ed. Engl.* **1984**, *23*, 579-586.
7. Bishop, K. C. *Chem. Rev.* **1976**, *76*, 461-486.
8. (a) For a review of Lewis acid-catalyzed isomerization of epoxides to carbonyl compounds, see: Rickborn, B. In *Comprehensive Organic Synthesis*; Trost, B. M., Ed.; Pergamon: Oxford, 1991; Vol. 3; Chapter 3.3, pp 733-775. (b) For representative examples of transition metal-catalyzed isomerization of epoxides to carbonyl compounds, see: Milstein, D.; Buchman, O.; Blum, J. *J. Org. Chem.* **1977**, *42*, 2299-2308 (Rh). Vankar, Y. D.; Chaudhuri, N. C.; Singh, S. P. *Synth. Commun.* **1986**, *16*, 1621-1626 (Pd). Visentin, G.; Piccolo, O.; Consiglio, G. *J. Mol. Catal.* **1990**, *61*, L1-L5 (Pd). Alper, H.; Des Roches, D.; Durst, T.; Legault, R. *J. Org. Chem.* **1976**, *41*, 3611-3613 (Mo). Prandi, J.; Namy, J. L.; Menoret, G.; Kagan, H. B. *J. Organomet. Chem.* **1985**, *285*, 449-460 (Mn, Ce, Sm). (c) For a review of base-promoted isomerization of epoxides to allylic alcohols, see: Crandall, J. K.; Apparau, M. *Org. React. (N. Y.)* **1983**, *29*, 345-443.
9. Kulasegaram, S.; Kulawiec, R. J. *J. Org. Chem.* **1994**, *59*, 7195-7196.
10. Kulasegaram, S.; Kulawiec, R. J. *J. Org. Chem.* **1997**, *62*, 6547-6561.
11. Kulasegaram, S.; Kulawiec, R. J. *Abstracts of Papers*, 213th National Meeting of the American Chemical Society, San Francisco, CA; American Chemical Society: Washington, DC, 1997; ORGN 0413.
12. Atwood, J. D. *Inorganic and Organometallic Reaction Mechanisms*; Brooks/Cole: Monterey, 1985; Chapter 1.
13. (a) Heck, R. F. *Palladium Reagents in Organic Synthesis*; Academic Press: London, 1985. (b) Trost, B. M.; Verhoeven, T. R. In *Comprehensive Organometallic Chemistry*; Wilkinson, G., Ed.; Pergamon: Oxford, 1982; Vol. 8; Chapter 57.
14. (a) Carpenter, B. K. *Determination of Organic Reaction Mechanisms*; Wiley & Sons: New York, 1984; Chapter 4. (b) See ref. 14a, pp 154-156. (c) See ref 14a, Chapter 5.
15. The formation of a highly nucleophilic Pd(0)-tertiary phosphine complex from Pd(OAc)<sub>2</sub> and PBu<sub>3</sub> is well-established. Although the precise molecular composition of the product formed has not been determined, its spectroscopic and chemical properties are fully consistent with the formulation Pd(PBu<sub>3</sub>)<sub>n</sub>, where n depends upon the number of equivalents of PBu<sub>3</sub> added. See: Mandai, T.; Matsumoto, T.; Tsuji, J.; Saito, S. *Tetrahedron Lett.* **1993**, *34*, 2513-2516.
16. For a review of oxidative addition reactions, see: Crabtree, R. H. *The Organometallic Chemistry of the Transition Metals*, 2nd ed.; Wiley: New York, 1994; Chapter 6.
17. Chock, P. B.; Halpern, J. *J. Am. Chem. Soc.* **1966**, *88*, 3511-3514.
18. Hart-Davis, A. J.; Graham, W. A. G. *Inorg. Chem.* **1970**, *9*, 2658-2663.
19. Jawad, J. K.; Puddephatt, R. J. *J. Chem. Soc., Dalton Trans.* **1977**, 1466-1469.
20. Ugo, R.; Pasini, A.; Fusi, A.; Cenini, S. *J. Am. Chem. Soc.* **1972**, *94*, 7364-7370.
21. For a discussion of this point, see: Kochi, J. K. *Organometallic Mechanisms and Catalysis*; Academic Press: New York, 1978; pp 161-162.
22. See, for example: Lau, K. S. Y.; Wong, P. K.; Stille, J. K. *J. Am. Chem. Soc.* **1976**, *98*, 5832-5840.

23. However, using palladium acetate-tributylphosphine as catalyst, epoxide **4** isomerizes in 30 minutes to give a 96% yield of 3-(2-naphthyl)-2-butanone.<sup>10</sup>
24. Reichardt, C. *Solvents and Solvent Effects in Organic Chemistry*, 2nd ed.; VCH: Weinheim, 1988.
25. (a) Pimentel, G. C.; McClellan, A. L. *The Hydrogen Bond*; W. H. Freeman: San Francisco, 1960. (b) Jeffrey, G. A. *An Introduction to Hydrogen Bonding*; Oxford: New York, 1997.
26. Jawad, J. K.; Puddephatt, R. J. *J. Organomet. Chem.* **1976**, *117*, 297-302.
27. (a) Collman, J. P.; Hegedus, L. S.; Norton, J. R.; Finke, R. G. *Principles and Applications of Organotransition Metal Chemistry*; University Science Books: Mill Valley, CA, 1987; pp 386-388. (b) Cross, R. J. In *The Chemistry of the Metal-Carbon Bond*; Hartley, F. R.; Patai, S., Eds.; Wiley: New York, 1985; Vol. 2, Chapter 8.
28. Calhorda, M. J.; Galvão, A. M.; Ünaleroglu, C.; Zlota, A. A.; Frolow, F.; Milstein, D. *Organometallics* **1993**, *12*, 3316-3325.
29. Kim, J.-H.; Kulawiec, R. J. *J. Org. Chem.* **1996**, *61*, 7656-7657.
30. Evans, J.; Schwártz, J.; Urquhart, P. W. *J. Organomet. Chem.* **1974**, *81*, C37-C39.
31. Egger, K. W. *Int. J. Chem. Kinet.* **1969**, *1*, 459-472.
32. For summaries of recent work describing the chemistry of transition metal enolate complexes, see: (a) Burkhardt, E. R.; Doney, J. J.; Slough, G. A.; Stack, J. M.; Heathcock, C. H.; Bergman, R. G. *Pure Appl. Chem.* **1988**, *60*, 1-6. (b) Paterson, I. In *Comprehensive Organic Synthesis*; Trost, B. M., Ed.; Pergamon Press: Oxford, 1991; Vol. 2, Chapter 1.9. (c) Rasley, B. T.; Rapta, M.; Kulawiec, R. J. *Organometallics* **1996**, *15*, 2852-2854, and references therein.
33. Burkhardt, E. R.; Bergman, R. G.; Heathcock, C. H. *Organometallics* **1990**, *9*, 30-44.
34. Veya, P.; Floriani, C.; Chiesi-Villa, A.; Rizzoli, C. *Organometallics* **1993**, *12*, 4899-4907.
35. (a) Ito, Y.; Nakatsuka, M.; Kise, N.; Saegusa, T. *Tetrahedron Lett.* **1980**, *21*, 2873-2876. (b) Sodeoka, M.; Ohrai, K.; Shibasaki, M. *J. Org. Chem.* **1995**, *60*, 2648-2649.
36. (a) Milstein, D. *J. Am. Chem. Soc.* **1982**, *104*, 5228-5229. (b) Milstein, D.; Calabrese, J. C. *J. Am. Chem. Soc.* **1982**, *104*, 3773-3774.